

SUPPLEMENTAL MATERIAL

Phosphoproteomics with Activated Ion Electron Transfer Dissociation

Nicholas M. Riley,^{1,2} Alexander S. Hebert,¹ Gerhard Dürnberger,^{4,5,6} Florian Stanek,⁴ Karl Mechtler,^{4,6} Michael S. Westphall,¹ and Joshua J. Coon^{1,2,3,7,*}

¹Genome Center of Wisconsin, Departments of ²Chemistry and ³Biomolecular Chemistry, University of Wisconsin-Madison, Madison, WI, 53706, USA

⁴Institute of Molecular Pathology (IMP), Campus-Vienna-Biocenter 1, A-1030 Vienna, Austria

⁵GMI, Gregor Mendel Institute of Molecular Plant Biology, Dr. Bohr Gasse 3, A-1030 Vienna, Austria

⁶IMBA, Institute of Molecular Biotechnology of the Austrian Academy of Sciences, Dr. Bohr Gasse 3, A-1030 Vienna, Austria

⁷Morgridge Institute for Research, Madison, Wisconsin, USA

*Corresponding author: jcoon@chem.wisc.edu

Supplemental Materials and Methods

Figure S1. Summary of phosphopeptide identifications compared to HCD.

Figure S2. Overlap in unique phosphopeptides identified with ETD, ETHcD, and AI-ETD (15W).

Figure S3. Comparing sequence coverage maps from ETD and AI-ETD for the z = 16 precursor of α -casein.

Figure S4. Structure of a partial sequence of (residues 36-143) α -casein.

SUPPLEMENTAL MATERIALS AND METHODS

Sample Preparation. Mouse brain lysates were prepared as described in the companion manuscript to this paper.¹ The same mouse brain lysate used in the companion manuscript was used for phosphopeptide enrichments described herein, making comparisons between the two possible, as discussed in the text. Briefly, 4 mg mouse brain was lysed and digested overnight with trypsin (Promega, Madison, WI). Following peptide desalting via solid phase extraction, phosphopeptides were enriched using MagResyn Ti-IMAC Ti⁴⁺-functionalized magnetic microspheres (ReSyn Biosciences, Edenvale, South Africa). Buffer A was 80% ACN with 6% trifluoroacetic acid (TFA), Buffer B was 80% ACN with 0.5 M glycolic acid, and Buffer C was 50% ACN with 1% ammonium hydroxide. 200 μ L of beads were washed three times with 1 mL Buffer A. Desalted peptides were resuspended in 1 mL Buffer A, combined with the washed magnetic beads, and shaken for 20 minutes at room temperature. The beads were then washed three times with 1 mL Buffer A, once with 1 mL 100% ACN, once with 1 mL Buffer B, and once more with 1 mL Buffer B. Phosphopeptides were eluted with 300 μ L Buffer C and this process was repeated for a total of two elution washes. Phosphopeptides were then dried, desalted, and resuspended in 30 μ L 0.2% formic acid (FA) prior to LC-MS/MS analyses.

LC-MS/MS. Liquid chromatography conditions were identical to those described in the companion manuscript, and modification to the MS system to enable AI-ETD are also thoroughly described there.¹ One microliter resuspended phosphopeptides was injected onto the column and gradient elution was performed at 325 nL/min, which increased from 0 to 6% B over 6 min, followed by an increase to 55% at 73 min, a ramp to 100% B at 74 min, and a wash at 100% B for the 6 min. The column was then re-equilibrated at 0% B for 10 min, for a total analysis of 90 minutes. Eluting peptides were ionized using a nanoelectrospray source held at +2 kV with respect to ground and the inlet capillary temperature was held at 275 °C. Survey scans of peptide precursors were collected from 300 – 1350 Th with an AGC target of 5,000,000, a maximum injection time of 50 ms, and a resolution of 60,000 at 200 m/z . Monoisotopic precursor selection was enabled for peptide isotopic distributions, precursors of $z = 2-6$ were selected for data-dependent MS/MS scans for 2 seconds of cycle time, and dynamic exclusion was set to 10 seconds with a ± 10 ppm window set around the precursor. Calibrated charge dependent ETD parameters were enabled to determine ETD reagent ion AGC and ETD reaction times,² and all MS/MS were mass analyzed in the Orbitrap with a resolution of 15,000 K at 200 m/z . The MS/MS AGC target value was set to 100,000 with a maximum injection time of 100 ms, and precursors were isolated with a 1.5 Th window using the quadrupole. Normalized collision energies (nce) of 35, 25, and 30 were set for ETcaD, EThcD, and HCD experiments, respectively, and AI-ETD laser powers were either 12 Watt (W) or 15 W, as indicated in the text. For AI-ETD+ analyses, AI-ETD was performed using 15 W output from the laser head, and product ions were transferred from the high pressure cell to the low pressure cell for 2 ms of IRMPD activation at 9 W before being shuttled back to the high pressure cell to be subsequently injected to the Orbitrap for mass analysis.

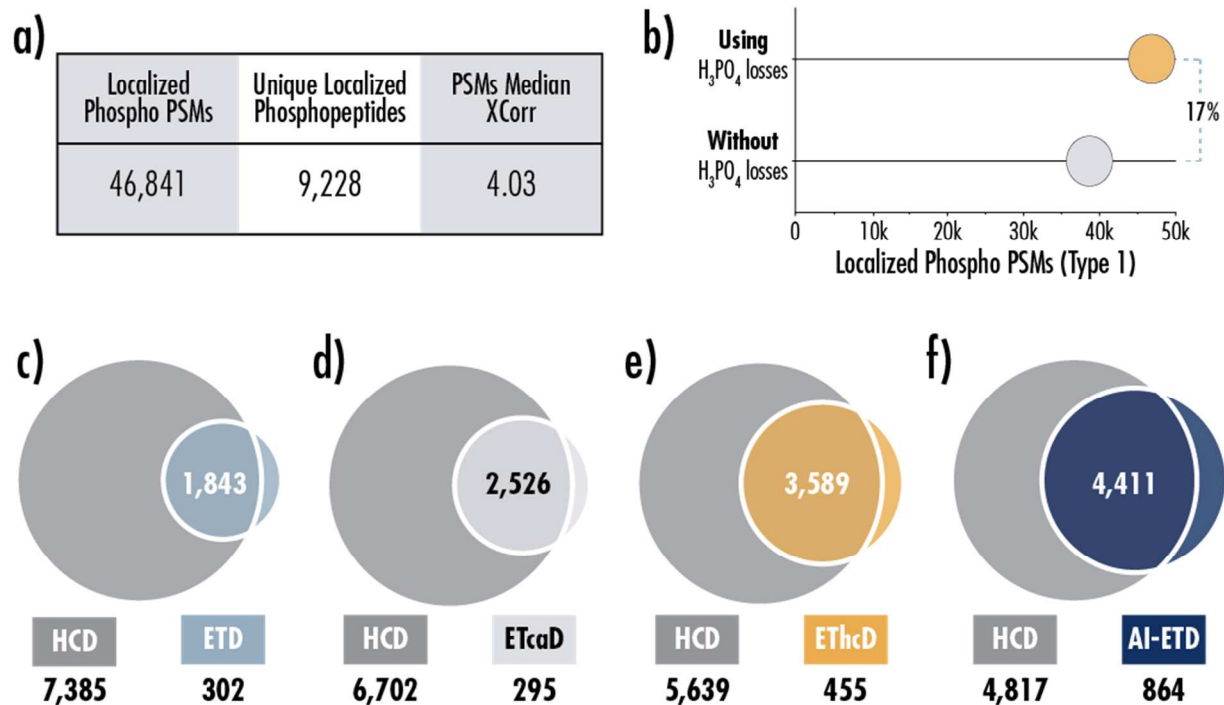
Bottom-Up Data Analysis. Tandem mass spectra were searched using Proteome Discoverer 1.4 software. Raw files were uploaded and the spectrum selector was used to select MS/MS spectra with precursor minimum and maximum set to 350 and 10,000 Da, respectively, and a peak filter set to a minimum signal-to-noise (S/N) threshold of 1.5. A non-fragment filter was applied, removing precursor peaks within a ± 1 Da window, charge reduced precursors with a ± 0.5 Da window, and neutral losses from the charge reduced precursor with a ± 0.5 Da window and a maximum neutral loss of 60 Da.^{3,4} The SEQUEST HT node was used to search spectra using a UniProt mouse (*mus musculus*) database (canonical and isoforms, downloaded May 12, 2016) with precursor mass tolerance of 50 ppm and a fragment mass tolerance of 0.2 Da.⁵

Fragment ion types searched were b-, y-, c-, and z-type for all but ETD where b-type were not included and HCD experiments where only b- and y-type fragments were used, and tryptic specificity was indicated. Carbamidomethylation of cysteine was set as a fixed modification, and oxidation of methionine and phosphorylation of serine, threonine, and tyrosine were set as variable modifications with a max of 4 equal modifications per peptide. The Percolator node was used to filter results to a 1% false discovery rate.^{6,7} phosphoRS version 3.1 was used to localize phosphosites with a 0.05 Da fragment mass tolerance,⁸ only phosphosites with localization probabilities of 75% and higher were considered as localized and used for further analysis, and the phosphoRS algorithm was modified to include phosphate neutral losses in ETD spectra as discussed in the text. Three technical replicate analyses were batched together for each method.

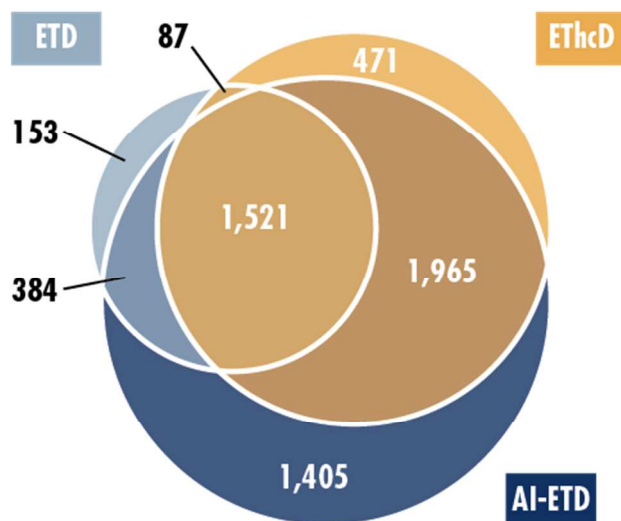
Top-Down Analysis. A-casein was purchased as a mass spectrometry grade standard from Protea Biosciences (Morgantown, WV) and was resuspended at 10 pmol/ μ L in 50% ACN / 49.8% H₂O, and 0.2% FA. The protein solution was infused via syringe pump into the mass spectrometer at 5 μ L/min using a 500 μ L syringe and precursors were ionized with electrospray ionization (ESI) at 4.5 kV with respect to ground. Intact protein mode was enabled to reduce nitrogen pressure in the ion-routing multipole to 3 mTorr, and full MS spectra were collected in the Orbitrap at a resolution of 240,000 K at 200 m/z with an AGC target value of 1,000,000. MS/MS scans were performed in the Orbitrap at a resolution of 240,000 at 200 m/z with an AGC target value of 800,000. Precursors were isolated with the mass selecting quadrupole using an isolation width of 5 m/z , and 200 transients were averaged. HCD collision energies ranged from 15-20 nce. An AGC target of 300,000 charges was used for fluoranthene reagent anions (m/z 202, isolated by the mass selecting quadrupole) for ETD, ETHcD, and AI-ETD experiments. ETD reaction times ranged from 12-30 ms depending on precursor charge state, ETHcD collision energies were either 12 or 15 nce, and AI-ETD laser powers were either 18 or 21 W. Multiple nce values and laser powers were tested for ETHcD and AI-ETD, respectively, to determine optimal performance (data not shown). MS/MS spectra were deconvoluted with XTRACT (Thermo Fisher Scientific) using default parameters and a S/N threshold of three. ProSight Lite was used to generate matched fragments using a 10 ppm tolerance.⁹ All ETD, ETHcD, and AI-ETD spectra were matched with c-, z-, b-, and y-type ions while HCD spectra were matched with b- and y-type fragments. Phosphoserines modified in α -casein were identified using known sites at the UniProt resource (accession P02663).

SUPPLEMENTAL REFERENCES

- (1) Riley, N. M.; Westphall, M. S.; Hebert, A. S.; Coon, J. J. *Anal. Chem.* **2017**, *submitted*.
- (2) Rose, C. M.; Rush, M. J. P.; Riley, N. M.; Merrill, A. E.; Kwiecien, N. W.; Holden, D. D.; Mullen, C.; Westphall, M. S.; Coon, J. J. *J. Am. Soc. Mass Spectrom.* **2015**, doi: 10.1007/s13361-015-1183-1.
- (3) Good, D. M.; Wenger, C. D.; McAlister, G. C.; Bai, D. L.; Hunt, D. F.; Coon, J. J. *J Am Soc Mass Spectrom* **2009**, *20*, 1435–1440.
- (4) Good, D. M.; Wenger, C. D.; Coon, J. J. *Proteomics* **2010**, *10*, 164–167.
- (5) Eng, J. K.; McCormack, A. L.; Yates, J. R. *J. Am. Soc. Mass Spectrom.* **1994**, *5*, 976–989.
- (6) Käll, L.; Canterbury, J. D.; Weston, J.; Noble, W. S.; MacCoss, M. J. *Nat. Methods* **2007**, *4*, 923–925.
- (7) Spivak, M.; Weston, J.; Bottou, L.; Käll, L.; Noble, W. S. *J. Proteome Res.* **2009**, *8*, 3737–3745.
- (8) Taus, T.; Köcher, T.; Pichler, P.; Paschke, C.; Schmidt, A.; Henrich, C.; Mechtler, K. *J. Proteome Res.* **2011**, *10*, 5354–5362.
- (9) Fellers, R. T.; Greer, J. B.; Early, B. P.; Yu, X.; LeDuc, R. D.; Kelleher, N. L.; Thomas, P. M. *Proteomics* **2014**.



Supplemental Figure 1. Summary of phosphopeptide identifications compared to HCD. a) The table provides the number of localized phospho PSMs and unique phosphopeptides identified with HCD. The median Xcorr of localized phospho PSMs from HCD analyses is also provided. **b)** Phosphate neutral loss ions are common in HCD spectra and losses from *b*- and *y*-type ions are used to help localize phosphosites in phosphoRS (gold). If these neutral losses in HCD spectra are not accounted for by the localization software, the number of confidently localized phospho PSMs by 17% (grey). **c-f)** The overlap in unique phosphopeptides identified with HCD and ETD (**c**), ETcID (**d**), EThcD (**e**), or AI-ETD (15W) (**f**) are shown.



Supplemental Figure 2. Overlap in unique phosphopeptides identified with ETD, EThcD, and AI-ETD (15W). AI-ETD identifies the large majority of phosphopeptides observed with the other two methods and adds more than 1,400 additional unique phosphopeptides to the identification pool.

ETD

89 matching fragments

36% sequence coverage

```
N  R P|K|H P|I|K|H|Q|G|L P|Q|E|V|L|N|E|N|L|L|R|F|F|V| 25
26 A P|F P|E|V|F|G|K|E|K|V|N E|L S|K|D I|G|S E|S T E| 50
51 D Q A M|E|D I|K|Q M|E A E S I S S S E E I V P N S 75
76 V|E Q K H|I|Q K|E|D|V P|S|E R Y L|G|Y L E|Q L L R 100
101|L|K K|Y|K|V P Q L E I V P N|S|A|E E R L H|S M K E 125
126 G I H|A Q Q K E P M I G V N|Q E L A Y F Y P E L F 150
151 R Q F Y Q L D A Y P S G A W Y Y V P L G T Q Y T D 175
176 A P S F S D I P|N P I G S E|N S E|K T T M|P L W C
```

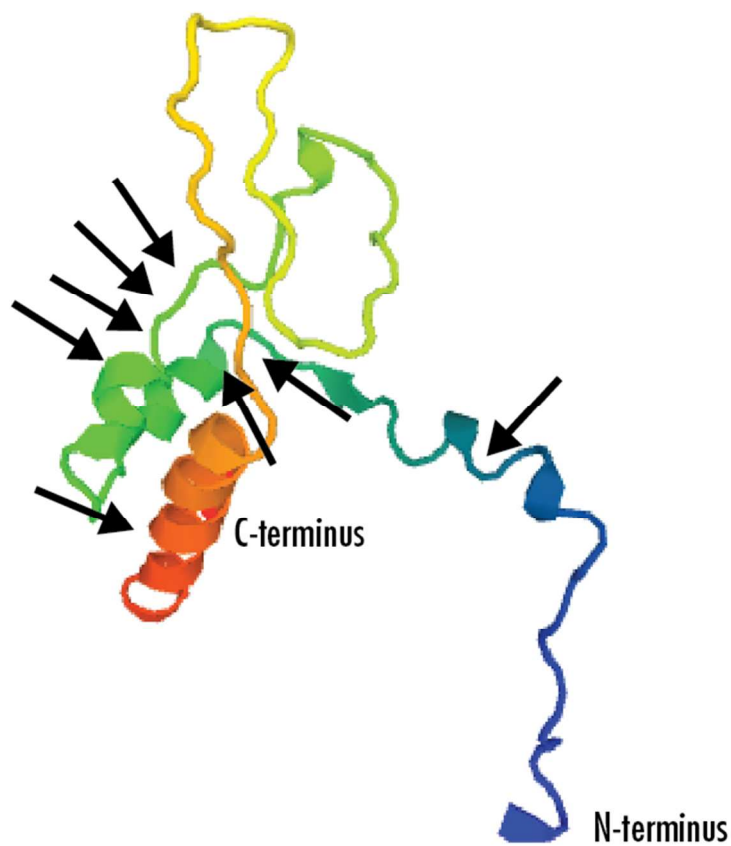
AI-ETD

143 matching fragments

58% sequence coverage

```
N  R P|K|H P|I|K|H|Q|G|L P|Q|E|V|L|N|E|N|L|L|R|F|F|V| 25
26 A P|F P|E|V|F|G|K|E|K|V|N E|L S|K|D I|G|S E|S T E| 50
51 D|Q|A M|E|D I|K|Q M|E A|E|S I S S S E E I V P N|S 75
76|V|E|Q K H I|Q K|E D V P|S|E|R|Y L|G|Y L E|Q|L L|R|100
101|L|K|K Y|K|V P Q L E I V P N|S|A|E|E|R L H|S M K E 125
126 G I H A Q|Q K|E P M I G V N Q E L A Y F Y P|E L F 150
151 R Q F Y Q L D A|Y P S G A W Y Y|V|P L|G|T|Q|Y|T|D 175
176|A|P|S|F|S|D|I P|N P I|G|S|E|N|S|E|K|T|T|M|P|L|W C
```

Supplemental Figure 3. Comparing sequence coverage maps from ETD and AI-ETD for the $z = 16$ precursor of α -casein. Interestingly, the N-terminal portion of the sequence is well characterized by both fragmentation methods, whereas AI-ETD provides more fragmentation in the middle and C-terminal regions of the protein. The structure of α -casein provides some insight into this behavior (**Figure S4**).



Supplemental Figure 4. Structure of a partial sequence of (residues 36-143) α -casein retrieved from the Protein Model Portal (<http://www.proteinmodelportal.org>) via Uniprot. The relatively linear N-terminal region is well characterized by both ETD and AI-ETD (**Figure S3**), while ETD provides minimal fragmentation in the C-terminal region that has more defined structure. AI-ETD improves fragmentation and sequence coverage in this region, supporting the concept of disruption of non-covalent interactions leading to better characterization with AI-ETD. Black arrows shows sites of phosphorylation. Note, α -casein was resuspended and electrosprayed in denaturing conditions, meaning any gas-phase structure that could have contributed to these differences may not be fully explained by in-solution structure as shown here.